WILEY-VCH

DOI: 10.1002/ ((please add manuscript number))
Progress Report

Ultrafast Field Emission Electron Source with Nanomaterials

Shenghan Zhou, Ke Chen, Matthew T. Cole, Zhenjun Li, Jun Chen, Chi Li, Qing Dai**

Mr. Shenghan Zhou, Mr. Ke Chen, Dr. Matthew T. Cole, Dr. Zhenjun Li, Dr. Chi Li, Prof. Qing Dai
Division of Nanophotonics, CAS Center for Excellence in Nanoscience, National Center for Nanoscience and Technology, Beijing 100190, China.
Email: daiq@nanoctr.cn (Q.D.), lichi@nanoctr.cn (C.L.)

Prof. Jun Chen
State Key Laboratory of Optoelectronic Materials and Technologies, Guangdong Province Key Laboratory of Display Material and Technology, School of Electronics and Information Technology, Sun Yat-sen University, Guangzhou 510275, China

Keywords: optical field emission, lightwave electronics, carbon nanotubes, two dimensional materials, ultrafast laser

The pursuit of simultaneous ultra-high spatial and temporal resolution electron sources are a subject of intense research for a wide variety of applications in emerging lightwave electronics and attosecond sciences. Recently, increasing research efforts on the production and integration of nanomaterials have projected wider scientific communities towards ultrafast electron emissiondevices that were hitherto manufacturable. Not only fascinating from the fundamental science point of view, such emerging electron emission systems offer an exciting platform for a wide variety of re-engineered as well as new applications. Here, the current state of the art in the field of ultrafast field electron emission, an in particular sub-optical-cycle field emission,

using nanostructures is reviewed. Metallic nanotips, carbon nanotubes, and silicon nanotips, along with other promising nanomaterial platforms are considered alongside possible future research fields such materials may open up.

1. Introduction

Electron sources lie at the heart of various ubiquitous and widely adopted systems; ranging from medical diagnosis to homeland security, electron emission systems find themselves at the very center of a wealth of technologies central to many industries. The first generation of vacuum electronic devices were bulky and slow thermionic sources, which continue to dominate the market more than a century after their inception. As new materials continue to emerge at pace, in the past few decades the electron emission community has increasingly shifted its focus towards cold cathode field electron emission[1]. Field induced electron emission is the quantum mechanical tunneling of electrons through a material dependent potential barrier under the influence of a high electric field. The absence of solid-state transport channel and the intrinsically ultrafast response time (attosecond) allow for near instantaneous emission resulting in much interest in various vacuum electronics devices such as flat panel display[2], microwave amplifiers[3], electron microscopy[4], and X-ray sources[5]. The successful demonstration of various nano-based field emission instruments is a significant milestone, which may ultimately lead to a combined spatial and temporal resolutions yet to be achieved using any other technology before them. The pursuit of high performance field emission source depends intimately on advanced materials engineering[6]. Nanomaterials have already demonstrated superior field emission performance compared to their bulk counterparts[7]. From ultra-low

excitation voltages, to extraordinarily high emission current densities, the distinctive electronic structures and nanometric emitting surfaces of these new materials imbue extremely high field enhancement factors[8]. Today, using nanomaterials, we can realize devices that simply could not be manufactured only a decade or so ago.

Commented [MC1]: Ref: **Achieving High-Current Carbon Nanotube Emitters**

However, the advantageous bifunctionality of field emission -- extremely high spatial and associated high temporal resolution -- has yet to fully capitalized on. In the past decade, motivated by attosecond science at sub-nanometric scale[9]; including the push towards ultrafast electron microscopy[10], next generation field emission electron sources with both sub-nanometer spatial resolution and attosecond temporal resolution have gained traction[11]. On one hand, much research remains in further enhancing the spatial resolution, typically achieved through the coupling of advanced transport physics and state-of-the-art materials science. By embracing bottom-up, atom-by-atom synthesis of new one-dimensional (1D)[12] and two dimensional (2D)[13-15] materials, the ultimate aim of engineering truly-single-atomic scale emission sites is becoming increasingly possible. Conversely, however, it is challenging to further improve the temporal resolution employing conventional driver electronics. New excitation methodologies are essential in order to reach femtosecond and even attosecond time scales. Excitation by ultrashort strong electromagnetic field of light is one viable candidate[16, 17]. It is this continuing pursuit of high temporal resolution field emission that has triggered the emergence of a new discipline - “lightwave electronics”,[18] whose central tenant is to investigate, and control, dynamic electron transport at sub-optical-cycle timescales.

Here we capture the present status of this emerging field. We first briefly review the methodologies associated with ultrafast field emission, including electric field and strong

optical field interactions. Then, we turn to the current development of ultrafast field emission electron sources and their applications, focusing on recent developments in optical field electron emission, mainly based on metal nanostructures alongside our recent progress on the production of carbon nanotube ultrafast emitters. Hereafter, we summarize the potential materials that will be interested for ultrafast field emission. This review aims to bridge the disciplines of conventional quasi statics field emission research and emerging ultrafast optical field emission research.

2. Ultrafast field emission methodology

2.1 Fundamentals of field emission

Classically, field electron emission is the quantum tunneling of electrons from an electron dense surface through a field augmented surface potential barrier, thereby allowing electrons to be emitted from a materials surface into a vacuum through a narrow potential barrier, typically achieved by the application of a high electric field. First modeled by Fowler and Nordheim in 1928,[19] in the case of metals metallic surfaces the emission current density J was found to depend on the electric field strength E, field enhancement factor β and the surface work function Φ, and has following form, commonly called the Fowler-Nordheim (F-N) Equation:

$$J = \frac{C_1(\beta E)^2}{\Phi} exp\left(-\frac{C_2 \Phi^{\frac{3}{2}}}{\beta E}\right),$$

Where $C_1 = \frac{e^3}{8\pi h}$, and $C_2 = \frac{8\pi\sqrt{2m}}{3he}$, are the basic constants (where e and m are the electron charge and the mass, respectively, and h is Plank's constant). Upon inspection it is clear that

Φ and β dominate the field emission characteristics of such electron dense materials. Though not explicitly true for all non-metallic systems, to date, a wide range of field emission materials have been studied, and regardless of the material type or dominant emission mechanism and associated emission model, a common methodology for emitter optimization and discovery has been, and continues to be, to decrease the surface barrier (work function Φ), and to regulate the external morphology of the material in order to increase the field emission enhancement factor.

2.2 Ultrafast laser assisted electric field emission

To improve the field emission performance, energy assisted electric field emission has been applied recently, including thermal-field emission[20] and photo-field emission[21] (Fig. 1A). In these regimes, electrons are first excited to higher energy levels by absorbing energy from thermal or optical excitation, allowing them to subsequently observe a much narrower tunneling barrier and hence allowing greater proportions of the electron population to more readily tunnel through the vacuum gap. Conventional energy assisted electric field emission employed electrical heating or laser exposure in order to provide this additional energy. However, though functional, thermal excitation methodologies do not readily allow for femtosecond response times.

Ultrafast femtosecond laser assisted electric field emission is the fore running candidate to retain, and ultimately exploit the ultrafast properties intrinsic to field emission[22]. Excited by exposure to ultrafast lasing, electrons may be excited to a nonequilibrium states, by obtaining energy from both photons and thermal (laser heating) affects. In the case of photon driven

excitation, the time scale of the general electron pulse is the same as the laser pulse[23]. Whilst, in the case of thermal driven excitation, time frames of >100 fs are required to transfer sufficient thermal energy to the local electron population[24].

2.3 Ultrafast optical field emission

Much faster field emission can be achieved by driving electron tunneling by strong electromagnetic fields, referred to as optical field emission (OFE)[25], as shown in Fig. 1B. This mechanism produces sub-optical-cycle duration electron pulses. Photoemission may transit into OFE from a conventional photon-driven regime, under a suitably strong optical field; a transition that can be described by the Keldysh framework.[26] Originally formulated for the ionization of a single atom, and latterly extended for photoemission from a metal surface,[27] Keldysh introduced a characteristic parameter γ that separates two limiting regimes; the multiphoton photoemission regime[28] ($\gamma > 1$) and the tunneling emission regime ($\gamma < 1$). The latter is termed OFE. The Keldysh parameter γ is given by $\gamma = \omega\sqrt{2m\phi}/e\beta F$, where ω is optical frequency, ϕ is work function, m is the mass of the electron and e is its charge, F is the incident light-field strengthen, β is the field enhancement factor of the emitting tips. During multiphoton photoemission (Fig. 1C), the minimum number n of the energy quanta $\hbar\omega$ required to overcome the work function are absorbed by the emitting surface ($\hbar$ is the reduced Planck constant). Here the photocurrent scales by a power law of the form I^n, where I refers to the laser intensity and the exponent n refers to the absorbed number of photons. In this photon-driven picture, more than the minimum required number of photons can be absorbed, resulting in what is termed above threshold mulitphoton photoemission[29] (Fig. 1D).

2.4 The nano advantage

Much of the research on field emission has, to date, relied on advances in materials technology, especially relating to nanomaterial growth and devices fabricated thereon. Ever increased field enhancement factors and consistently reduced work functions have proven key to lower the required external electric field and associated excitation laser intensity. Thus, smaller emitting tips fabricated from exotic materials continue to be pursued fervently. Longevity and brightness also stress the need for additional material properties, such as high mechanical strength, and low chemical reactivity, should such emitters operate successfully under common extreme conditions.

According to the Keldysh parameter (γ), to access OFE, high optical-field strengths are required. However, this is limited by both the materials' damage threshold as well as the available laser power. Thus, the optical near-field enhancement factor β of the emitter material plays a key role. β of 1D nanomaterials are mostly derived from the sharp tips induced "lightning rod effect", which also exists in static field emission[30]. At nanoscale discontinuities, such as nanotips, and nanorods, the electron density is notably very high, which induces highly enhanced near-field emission. Exploiting localized surface plasmons (LSPs) has proven a useful means of excitation and is a second excitation mechanism in near-field enhancement[31]. With resonant optical excitation, the system naturally leads to higher field enhancement than other mechanisms operating non-plasmonically[32].

Commented [MC2]: Is this the same beat as before? If no, perhaps we should call us beta with a subscript opt, or something like that in order to distinguish between them.

2.5 Experimental methods

Femtosecond laser exposure is required to achieve OFE due to the extremely high incident

optical field strength. Normally, an enhanced optical field strength of ~20 V/nm is necessary to access the OFE regime. For emitters with high field enhancement factor, the laser pulse intensity generated by comparatively inexpensive ultrafast oscillators with high repetition rates (MHz level) have proven sufficient to achieve strong field photoemission . However, if the field enhancement factor is low, ultrafast amplifiers are required, though such amplifiers often have deleteriously low repetition rates (KHz level) which contributes towards a reduced signal-to-noise ratio and ultimately poor functionality and a reduced number of potential applications The maximum photoemission current occurs when the optical polarization is parallel to the emitting tip axis. In order to collect the liberated electrons, a moderate static electric field is commonly applied between the tips and a counter electrode. We stress here that this DC field is not sufficiently large so as to extract the electrons directly by conventional DC electric field emission. The photoemission electron yield can be measured by a high precision digital source meter or counted by an electron multiplier plate. The emission image can be monitored by a phosphor screen, read out both electronically and by a timed and triggered charge-coupled device (CCD) camera to allow for spatial studies to be conducted. Finally, the energy distribution of the liberated electrons can be measured using, for example, a retarding field grid energy analyzer[ADD REFERENCE], time of flight spectrometer[ADD REFERENCE], or hemispherical energy analyzer[ADD REFERENCE]. The former two can reach an energy resolution of a few tens meV, while the latter can reach high resolution of a few meV.

OFE from nanotips is driven by the optical carrier waveform of the laser pulse rather than its envelop. To exam such behavior, careful control over the temporal evolution of the electric field of the laser pulses is required[33]. The use of ultrashort few-cycle pulses with control over their

Commented [MC3]: Add ref paper with an example that use this technique

Commented [MC4]: Add ref paper with an example that use this technique

Commented [MC5]: Please add a single reference to each of these

carrier envelop phase (CEP) are frequently used. The CEP of a laser pulse is the phase between the carrier wave (electric field) and its intensity envelope[34]. In a few-cycle laser pulse, the peak light-field of half-cycles (negative or positive cycles) can be sensitively controlled by tuning the CEP. For a nanotip emitter, OFE only occurs in half-cycles of the laser pulse, when the light-field direction is consistent with the tip orientation. The method exploits the exponential sensitivity of the emission probability on the field amplitude in combination with symmetry breaking at the emitting surface. CEP effects in photoemission can be used to realise CEP-based detectors[33, 35] and to reveal sub-optical-cycle dynamics associated with the photoemission process[36].

Commented [MC6]: Add reference to a paper that does this

3. State-of-the-art in ultrafast field electron emission sources

Research on ultrafast field emission has attracted huge interest, and this has led to significant progress over the past decade[34]. Many nanomaterials (including metal nanostructures, carbon nanomaterials, Si nanotips, and nano dielectrics) have been studied. Table 1 summarizes some now common ultrafast field emission materials and their key parameters. In this section, the current state-of-the-art in nanostructure-based ultrafast field emission sources is presented.

3.1 Metallic nanostructures

To date most of ultrafast field emission experiments have been conducted using metal materials due to their relatively simple electronic structures and strong plasmonic near-field enhancement. A variety of novel electron dynamics phenomena during OFE have been discovered from metal tips in this way. Metallic tips have already been applied in various practical devices, such as

Commented [MC7]: Provide three references that use metal nanostructures in their ultrafast FE work

ultrafast electron microscopy. In this section, we briefly review some of the novel electron dynamics observed on metal tips and their current application in ultrafast electron sources.

Recent research has demonstrated OFE from nanotips during short wavelength (<800 nm) excitation, which has proven a fundamental aspect in modern attosecond science due to its unique ability access ultra-fast physical and biological processes[16]. The transition into OFE was indicated by strong deviations of the photoemission transport profiles from the multiphoton photoemission power law[37, 38], as shown in Fig. 2A-C. However, such transitions are often observed at $1< \gamma<2$. This is inconsistent with the Keldshy theory[26], which predicted pure optical field emission at $\gamma \ll 1$. A hybrid photoemission regime is now widely accepted. At higher intensities, the light-field effect becomes increasingly dominant on the vacuum barrier, which results in the multiphoton photoemission channel closing[39]. Such an affect is theoretically predicted by the strong field approximation based on the time-dependent Schrödinger equation (Fig. 2D)[37]. It has been experimentally confirmed by electron spectroscopy that strong optical field shifted the high-order photoelectron peaks to lower kinetic energies alongside a closing of low-order channels[16], as shown in Fig. 2E. Further channel closing leads to a pronounced decrease of the effective nonlinearity to n~1[37], which has been observed at arrays of n-doped Si tips (800 nm) [40], Au nano-arrays (800 nm)[41], Au nano-array devices[42], CNTs (800 nm, 400 nm)[43, 44].

A novel quiver quenched electron dynamics was discovered in the OFE from Au nanotip[17]. Followed by tunneling into continuous states (first step), electrons will be accelerated in a strong optical near field (second step). This so-called two step Simpleman model captures the otherwise complex dynamics in a simplified form[45]. Despite simplicity, this model is capable

Commented [MC8]: Add reference to this work

Commented [MC9]: Is a name. Should be capitalized

Commented [MC10]: Add a reference to a paper that has accepted this hybrid model

to accurately describe various experimental observations. In the oscillating optical near field, the electrons have a typical quiver amplitude of $l_q = eF/m\omega^2$. In the case of nanoscale tips, the optical field decays exponentially with the distance from the tip surface, with a decay length l_F that is proportional to the tip radius. The electron trajectory is described by a spatial adiabaticity parameter ($\delta = l_F/l_q$). For δ>>1, most of the electrons quiver in the optical field, accompanied with strong surface rescattering, termed the quiver regime (upper panel of Fig. 3A and Fig. 3B). For δ<1, most of the emitting electrons escape the local optical field in one optical cycle, with minimized quiver and rescattering, termed the sub-cycle regime (lower panel of Fig. 3A and Fig. 3C). The sub-cycle regime encodes the instantaneous optical field, rather than its temporal integral, onto the electron energy. The locally accelerated electrons have excellent spatial coherence; critical for next generation ultrafast electron sources. The first observation of sub-optical-cycle acceleration in a nanotip near-field was presented by Ropers et al.[17] The effect has been further investigated in a systematic study by Echternkamp et al.[46] on W tip.

OFE of the metals is predicted to be very sensitive to the CEP [47], however, a low sensitivity to CEP modulation[48] has been observed in practice. As discussed previously, this is maybe due to limited optical-field modulation efficiency that resulted from the greatly reduced photoemission nonlinearity (i.e. power scaling of current-intensity curve). Another possible reason may include space charge effects[49] which induce photoemission current saturation. And hence, a lower sensitivity to modulation which may ultimately limit the range of practical applications, such as CEP detectors. Recently, the electron kinetic energy distributions of OFE from W tips has been noted to be more sensitive to the CEP. As discussed by Peter, et.al[16], the

cut-off energy of the spectrum comes from the electrons rescattering from the tips surface, which is strongly dependent on the maximum driven carrier field of the pulses, i.e. the CEP. The peaks in the energy distribution can be strongly modulated by CEP, and the modulation depths of the peak near the cut-off position reached up to 100%.

The ultrafast electron source of metallic tips have been applied in femtosecond point-projection microscopy (fsPPM),[57, 58] ultrafast low-energy electron diffraction (ULEED)[59] and combinations of the two.[60] This technology has extended the time resolution of electron microscopy to the picosecond and even femtosecond scale, however, the spatial resolution is limited to the order of hundred microns. In 2013, Barwick et al.[57] introduced nano ultrafast electron source into point-projection microscopy. They demonstrateda spatial resolution of 100 nm. When the spatial resolution is further reduced, it may replace expensive and complicated traditional electron microscopy systems. Following this, Gulde et al.[59], using W nanotips, developed a unique ULEED system with extremely high surface sensitivity to detect the surface structure of crystalline materials. Müller et al.[60] designed a compact hybrid device that combines fsPPM with femtosecond low-energy electron diffraction (fsLEED). The micro scale electron propagation distance greatly reduces the electron pulse broadening, while using single electron pulse to reach femtoseconds time resolution.

Besides metal nanotips, the effort to access the OFE regime were carried out with other specially designed nanostructures for higher enhancement effect, such as nanowires,[50] nanospheres,[51] nanorods,[52-54] nanotriangles,[42] nanostars,[55] and composite bow-tie antennae and nanorod antennae.[42, 56]

3.2 Carbon nanotubes

Based on the understanding of ultrafast field emission phenomenon from metallic tips, research has now extended into other materials in an attempt to exploit their advantages to the full. One promising class of materials are the carbon nanotubes (CNTs). Since the discovery of CNTs, they have gleaned unprecedented levels of attention across a wide range of applications, perhaps none more so intensely than as an electron source. These robust 1D materials are near ideal field electron emitters. A CNT may have an aspect ratio as high as 1000, some 10-100 times greater than an equivalent metallic emitters, and thus increase field enhancement factor. The enhancement of CNT is mostly based on geometrical effects, due to its extremely small tip radius. They also allow for very high field enhancement effect under much wider bandwidth. Recently, a very high enhancement factor of ~27 at 410 nm[44] and ~21 at 820 nm[43] were noticed in the first experiment of OFE from CNTs (Fig. 4A) with ~1 nm tip radius (Fig. 4B and 4C). The high optical field enhancement in the engineered CNTs allows, for the first time, access to field-driven photoemission at unprecedently short wavelengths of around 400 nm (Fig. 4D) with a corresponding β value of 26.7 (Figure 4(E)). In addition, the emitted electrons have great monochromaticity with energy spread as low as 0.25 eV (Fig. 4F).

As mentioned above, CNTs with sub-nanometric tips radius have an extremely small field decay length (<0.4 nm), which allows for easier access to quiver quenched electron dynamics in the OFE regime. However, the δ-parameter is inversely proportional to optical field (F) for a fixed wavelength. Because the experimentally accessible intensity range is limited by damage

thresholds, the access into sub-cycle regime by increasing F is expected to be somewhat less pronounced, especially for short wavelength excitation fields. Fortunately, CNT emitters have much higher β alongside a much smaller R compared with conventional metal tips, as well as a significantly greater damage threshold, all of which facilitate improved access into the sub-cycle regime[43]. In recent OFE experiment on multi-walled CNTs, δ decreased to a small value of ~0.53 with the laser power increasing. This suggests that OFE has accessed the sub-cycle regime effectively. This is also supported by the fact that the cut-off energy increases sub-linearly with the optical field strength. These demonstration opens exciting prospects for extending current characterization extreme to sub-femtosecond temporal resolution as well as sub-nanometer spatial resolution.

Commented [MC11]: WAS THIS A multi-walled cnt or not?

Commented [MC12]: ADD REFERNECE to this paper here

3.3 Other nanostructured ultrafast field emitters

In addition, Silicon nanotips array,[40] dielectric nanospheres,[61-64] metallic nanoclusters[65] and C_{60} "buckyballs",[66] carbon nanofibers[ref]. were used in strong-field experiments. For example, Swanwick et al.[40] designed arrays of nanosharp silicon pillars as a novel field emitter, achieving electron emission at low power. Passig et al.[65] investigated plasmon-enhanced photoemission from silver clusters. Li et al.[66] using few-cycle laser pulses demonstrate the spatiotemporal control of electronic wave packet motion in C_{60}. Moreover, many studies focus attention on dielectric nanospheres, including the attosecond control of the collective electron motion[61], electron scattering in strong-field photoemission,[63, 64] and CEP controlled photoemission.[62]

4. Potential ultrafast field emission materials.

A notably trend in the use of ever more exotic nanomaterials to investigate ultrafast field emission is currently under way. Besides their higher optical field enhancement factors, the potentially lower work functions are also preferred in order to reduce the required high optical field. In this section, we summarize the suitability and use of several potential nanomaterials as ultrafast field emitters.

4.1 Wide bandgap semiconductors

In order to seeking appropriate low work function materials for field emission, diamond thin films was discovered in the early 1990s[67]. It has attracted significant attention with many thousands of reports having been published to date. In addition to having low, and even negative surface electron affinity[68], diamond and related films are especially attractive emission platforms as they are chemically inert, and have extremely high thermal conductivity and mechanical toughness. Therefore, they are an excellent candidate for ultrafast field emission. However, the films have, due to their growth by nominally planar chemical vapor deposition methods, relatively low field enhancement factors which severely compromises their emission performance. Subsequently, diamond films or nanostructures[69] have also similarly been synthetized on other micro - nano tips to enhance the field emission properties of the uncoated materials[70].

The successful demonstration of excellent field emission of diamond and related materials led to the study of various wide bandgap semiconductors[71], including ZnO[72], WO_3[73], AlN[74],

SiC[75], GaN[76], BN[77], and SnO_2[78]. When nanostructured, these materials offer varied and unique emission properties. Among them, ZnO has been perhaps the most extensively studied, likely due to its ease of synthesis into tipped nanostructures at relatively low temperatures via hydrothermal processing, though vapor phase deposition methods are also widely adopted. Studied since 2002, the various sharp morphologies that can be produced by ZnO are wide ranging; from tetrapod's to nanowires[79].

4.2 Low work function materials

Perhaps the most successful low function materials to date, is Lanthanum hexaboride (LaB_6); widely used both in conventional electron microscopy and ultrafast electron microscopy, though other established materials include, RuO_2[80], and Cs[81]. The research on the use of LaB_6 as field emitter material has been an ongoing effort ever since 1960s [82]. As a cold field emitter, LaB_6 nanowires will offer a high emission current density mainly due to their low dimensionality, low work function (~2.6 eV), as well as excellent electrical, thermal, and mechanical properties. Compared with the conventional W emitter (φ = 4.5 eV), LaB_6 has a dramatically lower work function (φ = 2.5 eV)reducing the need for highly energetic excitation. Moreover, LaB_6 is 5-10 times harder than W, thereby improving its resistance against ion bombardment.[83] To obtain clean surface, Zhang et al.[84] propose a method which is field evaporation to fabricate single LaB_6 nanowires of different crystal orientations. They found that the <001> oriented LaB_6 nanowire emitter has the highest field emission symmetry, the <012> oriented LaB_6 nanowire has the lowest work function therefore possess the highest field emission intensity and the lowest emission energy spread. Field-emission measurements on a

Commented [MC13]: Not sure what we mean here.

single LaB_6 nanowire showed that a high emission current density of 5×10^5 A cm^{-2} was achieved at a voltage below 800 V with an effective emission area as small as 6.4 nm^2.[85] Furthermore, the field emission stability from the single LaB_6 nanowire emitter is significantly better than W cold field emitters. Recently, Zhang et al.[86] investigated a method of fabricating LaB_6 nanowires that emits electrons from a single point with high monochromaticity (Fig. 5A-C). This LaB_6 field emitter with nanostructured tip could emit at a high current density and extremely high stability. Benefitting from the low work function of 2.07 eV, the energy spread of the emitted electron is reduced considerably (Fig. 5D-E). All these make LaB_6 nanowires an excellent ultrafast field emitter.

4.3 Two-dimensional materials

Though a very wide variety of materials have been considered to date, it was not until the late 2000s that two-dimensional (2D) materials came to the fore in electron emission research. Graphene, the first widely studied 2D material gained much interest in this sense. Graphene is a single-layer of carbon atoms arranged in hexagonal lattices, which is well known for having broad application prospects due to its excellent thermal, mechanical and electrical properties.[87] Though nominally planar, and as such not immediately of use in morphology dependent electron emission, by carefully structuring its surface, graphene can be used to produced ultra-sharp tips that have a radius of curvature below 1 nm, and can thus produce the extremely high aspect ratios required for field electron emission. Cold field emission from graphene has been reported in the context of creating micro-fabricated nanometer-scale sharp protrusions to localize and enhance an applied electric field, either by transferring graphene sheets onto

Commented [MC14]: Add reference to matts small folded graphene nano fins paper on his website

metal/semiconductor nanotips,[88] graphene coating of Ni/Co nanotips,[89] or by forming vertically aligned graphene films.[90, 91] Some studies have demonstrated that thin carbon nanoflakes/nanosheets prepared by plasma-enhanced chemical vapor deposition (PEVCD)[92] show promising electron emission properties, such as low emission turn on voltage and large emission current density. Here we define the turn-on voltage defines the voltage required to produce an emission current of 1 nA, as widely accepted by the research community. Earlier, Cheng et al.[93] used the electrophoretic deposition technique to fabricate homogeneous single-layer graphene films, these films show excellent field-emission properties, with turn on field of 2.3 V/μm and threshold field of 5.2 V/μm, a large field enhancement factor of 3700, and good emission stability and uniformity. Soon afterwards, vertically aligned few-layer graphene was found to be a good field emitter by Malesevic et al.[94], characterized by turn on fields as low as 1 V/μm and field enhancement factors up to 7500, but which decays after only five cycles with the turn on field shifting to 3 V/μm and field enhancement factor decreasing to 3000. Such instabilities by means of tip degradation and surface augmentation continue to plague ultra-sharp emitted. A spin-coated graphene film was reported to exhibit a threshold field of 4 V/μm with a field enhancement factor of 1200.[91] And Rao et al.[95] fabricated undoped and doped graphene films synthesized by arc discharge in hydrogen, these high-density graphene films exhibit good field emission properties with a turn-on electric field of 0.7 V/μm. Recently, Wei et al.[96] reported a fast response surface electron emission from single atom graphene layer. Khursheed et al.[13] use a few-layer graphene-coated Ni wire point cathode to demonstrate that it is possible to obtain stable cold field emission for electron microscopy and lithography applications in high vacuum (HV) conditions and use relatively large point cathode tip

diameters, which is attributed to their experimentally measured ultralow work function of 1.1 eV.

MoS_2 is a naturally occurring molybdenite compound, when reduced to a single unit layer possesses interesting properties such as atomic sharp edges and unique electronic,[97] mechanical,[98] optical[99] properties. Earlier, Li et al.[100] have reported field emission properties of MoS_2 nanoflowers, synthesized by reducing the MoO_2 in sulfur environment, exhibiting a turn on field of 4.5–5.5 V/μm. Then, field emission from a few layer MoS_2 was first reported by Kashid et al.[101] at the base pressure of 1×10^{-8} mbar. For MoS_2 sheets, the turn on field required for a field emission current density of 10 $\mu A/cm^2$ is found to be 3.5 V/μm.

4.4 Molecule-scale emitters

Nanoscale hydrogen terminated carbon nanoparticles, or more commonly the Diamondoids, possess a variety of interesting and useful properties. Studies have shown that these unique macromolecules can produce monochromatic secondary electron emission,[102] due to their extraordinarily long carbon–carbon bonds[103]. It has been suggested that the novel electron emission noted from the Diamonoids is mediated by their negative electron affinity and small exciton binding energy caused by minimal quantum confinement in their unoccupied states.[104] They are interesting candidates for field emission because they represent the ultimate limit in diamond grain size reduction, which has previously been correlated with improved electron emission.[105] Melosh et al.[14] found that monolayers of diamondoids can effectively confer significantly enhanced field emission properties to metal surfaces, which was attributed to a reduction of the work function rather than a geometric enhancement. It is possible to transfer

the impressive field emission characteristics of diamond films to Au surfaces. In doing so it is possible to avoid transport issues relating to the low bulk diamond conductivity. Such hybrid systems are commonly realised by functionalizing Au surfaces with self-assembled monolayers (SAMs) of molecular-scale diamondoids. The four-cage tetramantane-thiol monolayers can reduce the work function of Au to 1.6–1.7 eV due to the formation of excited-state radical cations. This work proposes a new approach to modulate the surface work function using nanomaterials that form persistent radical cations rather than relying on reactive metals like Cs or Ru.

As the field of nanotechnology continues to progress, single atom and single molecule field emission sources are becoming manufacturable. Most recently, Esat et al.[12] reported a new molecular-scale electron emitter (Fig. 6A,B); a single molecule (3,4,9,10-perylenetetracarboxylic-dianhydride, PTCDA) standing on a metal surface that can emit electrons when excited by an electric field. They use the tip of a scanning tunnelling microscope to assemble a large planar aromatic molecules on silver surfaces. , With all prior studies noting this molecule lying with its long axis parallel to the planar metallic substrate, this atypical and surprisingly stable upright molecular orientation enables the system to function as a coherent single electron field emitter (Fig. 6C)which may indeed allow such designable molecules to usher in a generation of new macro-molecular electron sources that complement the library of nanowires and nanotubes currently available,[106] . If other metastable adsorbate configurations become available, it may well soon be possible to access a third spatial dimension for the design of functional nanostructures on surfaces.

5. Conclusion and outlook

Ultrafast field emission from nanomaterials is now becoming a very hot topic as it continues to be the vehicle that moves novel ultrafast electron dynamics beyond conventional knowledge and devices. The ability to produce ultrafast short electron pulses, driven by short wavelength (<800 nm) optical fields, has led to wide applications in the emerging field of lightwave electronics and attosecond sciences.

Though significant progress has been made, however, there remain many challenges plaguing the technology. For instance, an intrinsic physics problem in attosecond science arises from relating to the limiting frequency of OFE - how short can an electron pulse ultimately go? Although much work has been devoted to measuring the time of electron tunneling, only recently has experimental evidence come to the fore to suggest that this may be at the attosecond timescale[107], though the exact transit time remains unclear. Nevertheless, much exciting research remains to be undertaken here with particular focus on the ultimate limits of modern nanoscale mediated optoelectronics. OFE may eventually provide direct experimental evidence of this near ultimate technological limit in scale and speed. To this end, electron quiver in the near-field must be quenched as it induces a delayed photoemission process and further research into this is needed[108]. Thus, in the pursuit of quiver quenched OFE, research agendas focusing on the production of extremely sharp tips must be undertaken in order to reach extreme short near field decay lengths. Nonetheless, of all the emission mechanisms outlined here, certainly quiver quenched OFE shows the most potential in advancing the state of the art in advanced metrology and wider industrially viable electron emission devices. To date, of the wide

catalogue of bulk, 1D and 2D materials studied for use in electron emission systems, single wall CNTs are one of the few qualified materials for such a paradigm shifting purpose; these class-leading nanomaterials have emission sites principally located at ultra-small features at the tip but also at lattice defects. As the same concept, single atom and molecular emitters and single atomic layer materials based emitters are proving increasingly qualified, though present challenges with their mass and reproducible production make them somewhat more distant from application than the CNTs.

When accessing the OFE regime under short wavelengthexcitation, nonlinearity is greatly reduced and the optical field modulation efficiency is limited, both of which have hampered its practical application in attosecond devices, such as CEP detectors, to date. Present OFE is a hybrid process in which the strong optical field vibrates the vacuum barrier and results in multiphoton channel closing effect[16, 37], rather than a pure optical tunneling from states within the vicinity of the Fermi level. There remains much technology centered research exloring the potential tofurther increase the optical field strength in order to access the pure optical field emission regime, and thereby achieving much higher nonlinearity with the the photoemission current exhibiting an exponentially increasing trend with intensity. However, this requires nano and sub-nanoscale ultra-sharp emitting tips which not only have a higher optical field enhancement, but also all us to avoid space-charge effects[49, 109], another key constraint. Certainly, it would seem that the use of sub-nanometric CNTs tip offers and exciting potential route for the advancement of lightwave electronics.

As the general physics picture of ultrafast electron emission continues to take shape, most central tenants to this framework have been established using metallic nanotips. There is a clear

need for revision of these for the emerging nanomaterials, with a clear focus on introducing further research on the effects of distinctive electronic band structures of these new materials. For instance, the highly tunable electronic structure of CNTs by charity, chemical doping, and electrical gating - to name but a few - are additional important controllable factors for novel OFE electron dynamics that need careful consideration and study. For this purpose, examination of single sub-nanometric CNT tips for highly coherent ultrafast electron source is essential. Greatly reducing the emitter surface work function is another alternative way to facilitate the access into OFE, which has proven the preserve of many research groups, particularly relating to the work for LaB_6, diamond, and other wide bandgap materials. Their band structures will of course trigger novel interband and intraband electron dynamics[110], which greatly affect the emission performance and as such warrants additional further broad study.

Field emission, though considered by many to be a bygone research field is returning to the fore with vigour. By marrying advances in materials synthesis with recent developments in optics, new and exciting research, devices, technologies, and commercial opportunities abound this new field of study in the coming decade.

Acknowledgements

S.Z. and K.C. contributed equally to this work. We acknowledge funding from the National Key R&D Program of China (grant no. 2016YFA0202001), the National Natural Science Foundation of China (grant no. 11427808). Q.D. also benefited greatly from many international collaborators, specifically Prof. Kaihui Liu in Peking University, Prof. Zhipei Sun in Aalto University, Prof. Sheng Meng in Institute of Physics Chinese Academy of Sciences, Prof. Jiayu Dai and Prof. Xiaowei Wang in National University of Defense Technoloy.

Conflict of Interest

The authors declare no conflict of interest.

References

[1] N. S. Xu, S. E. Huq, *Materials Science and Engineering: R: Reports* **2005**, *48*, 47.

[2] W. B. Choi, D. S. Chung, J. H. Kang, H. Y. Kim, Y. W. Jin, I. T. Han, Y. H. Lee, J. E. Jung, N. S. Lee, G. S. Park, J. M. Kim, *Appl Phys Lett* **1999**, *75*, 3129; Q. H. Wang, A. A. Setlur, J. M. Lauerhaas, J. Y. Dai, E. W. Seelig, R. P. H. Chang, *Appl Phys Lett* **1998**, *72*, 2912.

[3] D. R. Whaley, B. M. Gannon, C. R. Smith, C. M. Armstrong, C. A. Spindt, *Ieee T Plasma Sci* **2000**, *28*, 727; W. I. Milne, K. B. K. Teo, E. Minoux, O. Groening, L. Gangloff, L. Hudanski, J. P. Schnell, D. Dieumegard, F. Peauger, I. Y. Y. Bu, M. S. Bell, P. Legagneux, G. Hasko, G. A. J. Amaratunga, *J Vac Sci Technol B* **2006**, *24*, 345.

[4] R. Aihara, H. Saito, H. Kohinata, K. Ogura, H. Otsugi, *J Electron Microsc* **1978**, *27*, 353.

[5] G. Cao, Y. Z. Lee, R. Peng, Z. Liu, R. Rajaram, X. Calderon-Colon, L. An, P. Wang, T. Phan, S. Sultana, D. S. Lalush, J. P. Lu, O. Zhou, *Phys Med Biol* **2009**, *54*, 2323; Z. J. Liu, G. Yang, Y. Z. Lee, D. Bordelon, J. P. Lu, O. Zhou, *Appl Phys Lett* **2006**, *89*.

[6] W. A. Deheer, A. Chatelain, D. Ugarte, *Science* **1995**, *270*, 1179.

[7] A. G. Rinzler, J. H. Hafner, P. Nikolaev, L. Lou, S. G. Kim, D. Tomanek, P. Nordlander, D. T. Colbert, R. E. Smalley, *Science* **1995**, *269*, 1550.

[8] T. Y. Zhai, L. Li, Y. Ma, M. Y. Liao, X. Wang, X. S. Fang, J. N. Yao, Y. Bando, D. Golberg, *Chem Soc Rev* **2011**, *40*, 2986.

[9] H. Niikura, P. B. Corkum, *Adv Atom Mol Opt Phy* **2007**, *54*, 511; P. B. Corkum, F. Krausz, *Nat Phys* **2007**, *3*, 381; M. F. Ciappina, J. A. Perez-Hernandez, A. S. Landsman, W. A. Okell, S. Zherebtsov, B. Foerg, J. Schoetz, L. Seiffert, T. Fennel, T. Shaaran, T. Zimmermann, A. Chacon, R. Guichard, A. Zair, J. W. G. Tisch, J. P. Marangos, T. Witting, A. Braun, S. A. Maier, L. Roso, M. Kruger, P. Hommelhoff, M. F. Kling, F. Krausz, M. Lewenstein, *Rep Prog Phys* **2017**, *80*.

[10] B. Barwick, H. S. Park, O. H. Kwon, J. S. Baskin, A. H. Zewail, *Science* **2008**, *322*, 1227; A. Feist, K. E. Echternkamp, J. Schauss, S. V. Yalunin, S. Schaefer, C. Ropers, *Nature* **2015**, *521*, 200; A. Ryabov, P. Baum, *Science* **2016**, *353*, 374.

[11] A. Feist, N. Bach, N. R. da Silva, T. Danz, M. Moller, K. E. Priebe, T. Domrose, J. G. Gatzmann, S. Rost, J. Schauss, S. Strauch, R. Bormann, M. Sivis, S. Schafer, C. Ropers, *Ultramicroscopy* **2017**, *176*, 63; D. Ehberger, J. Hammer, M. Eisele, M. Kruger, J. Noe, A. Hogele, P. Hommelhoff, *Phys Rev Lett* **2015**, *114*.

[12] T. Esat, N. Friedrich, F. S. Tautz, R. Temirov, *Nature* **2018**, *558*, 573.

[13] X. Y. Shao, A. Srinivasan, W. K. Ang, A. Khursheed, *Nat. Commun.* **2018**, *9*, 8.

[14] K. T. Narasimha, C. H. Ge, J. D. Fabbri, W. Clay, B. A. Tkachenko, A. A. Fokin, P. R. Schreiner, J. E. Dahl, R. M. K. Carlson, Z. X. Shen, N. A. Melosh, *Nat. Nanotechnol.* **2016**, *11*, 267.

[15] L. Iemmo, A. Di Bartolomeo, F. Giubileo, G. Luongo, M. Passacantando, G. Niu, F. Hatami, O. Skibitzki, T. Schroeder, *Nanotechnology* **2017**, *28*.

[16] M. Krueger, M. Schenk, P. Hommelhoff, *Nature* **2011**, *475*, 78.

[17] G. Herink, D. R. Solli, M. Gulde, C. Ropers, *Nature* **2012**, *483*, 190.

[18] E. Goulielmakis, V. S. Yakovlev, A. L. Cavalieri, M. Uiberacker, V. Pervak, A. Apolonski, R. Kienberger, U.

Kleineberg, F. Krausz, *Science* **2007**, *317*, 769.
[19] R. H. Fowler, L. Nordheim, *Proceedings of the Royal Society of London Series a-Containing Papers of a Mathematical and Physical Character* **1928**, *119*, 173; E. L. Murphy, R. H. Good, *Physical Review* **1956**, *102*, 1464.
[20] C. Li, Z. Li, C. Ke, B. Bing, D. Qing, *Appl Phys Lett* **2017**, *110*; Z. J. Li, B. Bai, C. Li, Q. Dai, *Carbon* **2016**, *96*, 641.
[21] R. Ganter, R. Bakker, C. Gough, S. C. Leemann, M. Paraliev, M. Pedrozzi, F. Le Pimpec, V. Schlott, L. Rivkin, A. Wrulich, *Phys Rev Lett* **2008**, *100*.
[22] D. Ehberger, J. Hammer, M. Eisele, M. Krueger, J. Noe, A. Hoegele, P. Hommelhoff, *Phys Rev Lett* **2015**, *114*.
[23] P. Hommelhoff, C. Kealhofer, M. A. Kasevich, *Phys Rev Lett* **2006**, *97*.
[24] B. Barwick, C. Corder, J. Strohaber, N. Chandler-Smith, C. Uiterwaal, H. Batelaan, *New Journal of Physics* **2007**, *9*.
[25] P. Hommelhoff, Y. Sortais, A. Aghajani-Talesh, M. A. Kasevich, *Phys Rev Lett* **2006**, *96*; H. Yanagisawa, C. Hafner, P. Dona, M. Klockner, D. Leuenberger, T. Greber, M. Hengsberger, J. Osterwalder, *Phys Rev Lett* **2009**, *103*.
[26] L. V. Keldysh, *Soviet Physics Jetp-Ussr* **1965**, *20*, 1307.
[27] F. V. Bunkin, M. V. Fedorov, *Soviet Physics Jetp-Ussr* **1965**, *21*, 896.
[28] P. Musumeci, L. Cultrera, M. Ferrario, D. Filippetto, G. Gatti, M. S. Gutierrez, J. T. Moody, N. Moore, J. B. Rosenzweig, C. M. Scoby, G. Travish, C. Vicario, *Phys Rev Lett* **2010**, *104*.
[29] L. Seiffert, T. Paschen, P. Hommelhoff, T. Fennel, *J Phys B-at Mol Opt* **2018**, *51*.
[30] M. S. Xue, W. F. Wang, J. F. Ou, F. J. Wang, W. Li, *Appl Phys Lett* **2013**, *102*.
[31] E. Betzig, J. K. Trautman, *Science* **1992**, *257*, 189.
[32] P. F. Liao, A. Wokaun, *J Chem Phys* **1982**, *76*, 751.
[33] G. G. Paulus, F. Lindner, H. Walther, A. Baltuska, E. Goulielmakis, M. Lezius, F. Krausz, *Phys Rev Lett* **2003**, *91*.
[34] T. Wittmann, B. Horvath, W. Helml, M. G. Schatzel, X. Gu, A. L. Cavalieri, G. G. Paulus, R. Kienberger, *Nat Phys* **2009**, *5*, 357.
[35] G. G. Paulus, F. Grasbon, H. Walther, P. Villoresi, M. Nisoli, S. Stagira, E. Priori, S. De Silvestri, *Nature* **2001**, *414*, 182; T. Wittmann, B. Horvath, W. Helml, M. G. Schaetzel, X. Gu, A. L. Cavalieri, G. G. Paulus, R. Kienberger, *Nat Phys* **2009**, *5*, 357.
[36] F. Lindner, M. G. Schatzel, H. Walther, A. Baltuska, E. Goulielmakis, F. Krausz, D. B. Milosevic, D. Bauer, W. Becker, G. G. Paulus, *Phys Rev Lett* **2005**, *95*; R. Gopal, K. Simeonidis, R. Moshammer, T. Ergler, M. Duerr, M. Kurka, K. U. Kuehnel, S. Tschuch, C. D. Schroeter, D. Bauer, J. Ullrich, A. Rudenko, O. Herrwerth, T. Uphues, M. Schultze, E. Goulielmakis, M. Uiberacker, M. Lezius, M. F. Kling, *Phys Rev Lett* **2009**, *103*.
[37] R. Bormann, M. Gulde, A. Weismann, S. V. Yalunin, C. Ropers, *Phys Rev Lett* **2010**, *105*.
[38] M. E. Swanwick, P. D. Keathley, A. Fallahi, P. R. Krogen, G. Laurent, J. Moses, F. X. Kartner, L. F. Velasquez-Garcia, *Nano Lett.* **2014**, *14*, 5035; R. G. Hobbs, Y. Yang, A. Fallahi, P. D. Keathley, E. De Leo, F. X. Kaertner, W. S. Graves, K. K. Berggren, *Acs Nano* **2014**, *8*, 11474.
[39] M. Kruger, M. Schenk, M. Forster, P. Hommelhoff, *J Phys B-at Mol Opt* **2012**, *45*.
[40] M. E. Swanwick, P. D. Keathley, A. Fallahi, P. R. Krogen, G. Laurent, J. Moses, F. X. Kaertner, L. F. Velasquez-Garcia, *Nano Lett.* **2014**, *14*, 5035.
[41] R. G. Hobbs, Y. Yang, P. D. Keathley, M. E. Swanwick, L. F. Velasquez-Garcia, F. X. Kartner, W. S. Graves, K. K. Berggren, *Nanotechnology* **2014**, *25*.

[42] W. P. Putnam, R. G. Hobbs, P. D. Keathley, K. K. Berggren, F. X. Kaertner, *Nat Phys* **2017**, *13*, 335.
[43] C. Li, X. Zhou, F. Zhai, Z. Li, F. Yao, R. Qiao, K. Chen, D. Yu, Z. Sun, K. Liu, Q. Dai, *Appl Phys Lett* **2017**, *111*, 133101.
[44] C. Li, X. Zhou, F. Zhai, Z. J. Li, F. R. Yao, R. X. Qiao, K. Chen, M. T. Cole, D. P. Yu, Z. P. Sun, K. H. Liu, Q. Dai, *Adv. Mater.* **2017**, *29*, 6.
[45] P. B. Corkum, *Phys Rev Lett* **1993**, *71*, 1994.
[46] K. E. Echternkamp, G. Herink, S. V. Yalunin, K. Rademann, S. Schafer, C. Ropers, *Appl. Phys. B-Lasers Opt.* **2016**, *122*, 10.
[47] C. Lemell, X. M. Tong, F. Krausz, J. Burgdorfer, *Phys Rev Lett* **2003**, *90*; M. I. Stockman, P. Hewageegana, *Appl. Phys. A* **2007**, *89*, 247.
[48] A. Apolonski, P. Dombi, G. G. Paulus, M. Kakehata, R. Holzwarth, T. Udem, C. Lemell, K. Torizuka, J. Burgdorfer, T. W. Hansch, F. Krausz, *Phys Rev Lett* **2004**, *92*; P. Racz, S. E. Irvine, M. Lenner, A. Mitrofanov, A. Baltuska, A. Y. Elezzabi, P. Dombi, *Appl Phys Lett* **2011**, *98*.
[49] B. Piglosiewicz, *Nat Photonics* **2014**, *8*, 79.
[50] B. Ahn, J. Schötz, M. Kang, W. A. Okell, S. Mitra, B. Förg, S. Zherebtsov, F. Süßmann, C. Burger, M. Kübel, C. Liu, A. Wirth, E. Di Fabrizio, H. Yanagisawa, D. Kim, B. Kim, M. F. Kling, *APL Photonics* **2017**, *2*, 036104.
[51] F. Schertz, M. Schmelzeisen, M. Kreiter, H.-J. Elmers, G. Schoenhense, *Phys Rev Lett* **2012**, *108*.
[52] Q. Sun, K. Ueno, H. Yu, A. Kubo, Y. Matsuo, H. Misawa, *Light-Science & Applications* **2013**, *2*.
[53] F. Kusa, K. E. Echternkamp, G. Herink, C. Ropers, S. Ashihara, *Aip Advances* **2015**, *5*.
[54] M. Lehr, B. Foerster, M. Schmitt, K. Kruger, C. Sonnichsen, G. Schonhense, H.-J. Elmers, *Nano Lett.* **2017**, *17*, 6606.
[55] M. Sivis, N. Pazos-Perez, R. Yu, R. Alvarez-Puebla, F. J. García de Abajo, C. Ropers, *Communications Physics* **2018**, *1*.
[56] P. Dombi, A. Hoerl, P. Racz, I. Marton, A. Truegler, J. R. Krenn, U. Hohenester, *Nano Lett.* **2013**, *13*, 674; T. Rybka, M. Ludwig, M. F. Schmalz, V. Knittel, D. Brida, A. Leitenstorfer, *Nat Photonics* **2016**, *10*, 667; R. G. Hobbs, W. P. Putnam, A. Fallahi, Y. Yang, F. X. Kaertner, K. K. Berggren, *Nano Lett.* **2017**, *17*, 6069; P. Racz, Z. Papa, I. Marton, J. Budai, P. Wrobel, T. Stefaniuk, C. Prietl, J. R. Krenn, P. Dombi, *Nano Lett.* **2017**, *17*, 1181.
[57] E. Quinonez, J. Handali, B. Barwick, *Rev. Sci. Instrum.* **2013**, *84*, 7.
[58] A. R. Bainbridge, C. W. B. Myers, W. A. Bryan, *Struct. Dyn.-US* **2016**, *3*, 16.
[59] M. Gulde, S. Schweda, G. Storeck, M. Maiti, H. K. Yu, A. M. Wodtke, S. Schafer, C. Ropers, *Science* **2014**, *345*, 200.
[60] M. Muller, A. Paarmann, R. Ernstorfer, *Nat. Commun.* **2014**, *5*, 8.
[61] S. Zherebtsov, T. Fennel, J. Plenge, E. Antonsson, I. Znakovskaya, A. Wirth, O. Herrwerth, F. Suessmann, C. Peltz, I. Ahmad, S. A. Trushin, V. Pervak, S. Karsch, M. J. J. Vrakking, B. Langer, C. Graf, M. I. Stockman, F. Krausz, E. Ruehl, M. F. Kling, *Nat Phys* **2011**, *7*, 656.
[62] F. Suessmann, L. Seiffert, S. Zherebtsov, V. Mondes, J. Stierle, M. Arbeiter, J. Plenge, P. Rupp, C. Peltz, A. Kessel, S. A. Trushin, B. Ahn, D. Kim, C. Graf, E. Ruehl, M. F. Kling, T. Fennel, *Nat. Commun.* **2015**, *6*.
[63] L. Seiffert, P. Henning, P. Rupp, S. Zherebtsov, P. Hommelhoff, M. F. Kling, T. Fennel, *Journal of Modern Optics* **2017**, *64*, 1096.
[64] L. Seiffert, Q. Liu, S. Zherebtsov, A. Trabattoni, P. Rupp, M. C. Castrovilli, M. Galli, F. Suessmann, K. Wintersperger, J. Stierle, G. Sansone, L. Poletto, F. Frassetto, I. Halfpap, V. Mondes, C. Graf, E. Ruehl, F. Krausz, M. Nisoli, T. Fennel, F. Calegari, M. F. Kling, *Nat Phys* **2017**, *13*, 766.
[65] J. Passig, S. Zherebtsov, R. Irsig, M. Arbeiter, C. Peltz, S. Goede, S. Skruszewicz, K.-H. Meiwes-Broer, J. Tiggesbaeumker, M. F. Kling, T. Fennel, *Nat. Commun.* **2017**, *8*.

[66] H. Li, B. Mignolet, G. Wachter, S. Skruszewicz, S. Zherebtsov, F. Suessmann, A. Kessel, S. A. Trushin, N. G. Kling, M. Kuebel, B. Ahn, D. Kim, I. Ben-Itzhak, C. L. Cocke, T. Fennel, J. Tiggesbaeumker, K. H. Meiwes-Broer, C. Lemell, J. Burgdoerfer, R. D. Levine, F. Remacle, M. F. Kling, *Phys Rev Lett* **2015**, *114*.

[67] M. W. Geis, N. N. Efremow, J. D. Woodhouse, M. D. Mcaleese, M. Marchywka, D. G. Socker, J. F. Hochedez, *Ieee Electr Device L* **1991**, *12*, 456.

[68] J. Vanderweide, Z. Zhang, P. K. Baumann, M. G. Wensell, J. Bernholc, R. J. Nemanich, *Phys Rev B* **1994**, *50*, 5803.

[69] N. G. Shang, P. Papakonstantinou, P. Wang, A. Zakharov, U. Palnitkar, I. N. Lin, M. Chu, A. Stamboulis, *Acs Nano* **2012**, *6*, 7540.

[70] T. Tyler, V. V. Zhirnov, A. V. Kvit, D. Kang, J. J. Hren, *Appl Phys Lett* **2003**, *82*, 2904.

[71] W. K. Yi, T. Jeong, S. G. Yu, J. Heo, C. Lee, J. Lee, W. Kim, J. B. Yoo, J. Kim, *Adv. Mater.* **2002**, *14*, 1464.

[72] F. H. Chu, C. W. Huang, C. L. Hsin, C. W. Wang, S. Y. Yu, P. H. Yeh, W. W. Wu, *Nanoscale* **2012**, *4*, 1471.

[73] F. Liu, L. Li, F. Y. Mo, J. Chen, S. Z. Deng, N. S. Xu, *Cryst Growth Des* **2010**, *10*, 5193.

[74] J. H. He, R. S. Yang, Y. L. Chueh, L. J. Chou, L. J. Chen, Z. L. Wang, *Adv. Mater.* **2006**, *18*, 650.

[75] Z. W. Pan, H. L. Lai, F. C. K. Au, X. F. Duan, W. Y. Zhou, W. S. Shi, N. Wang, C. S. Lee, N. B. Wong, S. T. Lee, S. S. Xie, *Adv. Mater.* **2000**, *12*, 1186.

[76] B. D. Liu, Y. Bando, C. C. Tang, F. F. Xu, J. Q. Hu, D. Golberg, *J Phys Chem B* **2005**, *109*, 17082.

[77] X. X. Yang, Z. J. Li, F. He, M. J. Liu, B. Bai, W. Liu, X. Qiu, H. Zhou, C. Li, Q. Dai, *Small* **2015**, *11*, 3710.

[78] H. Chi, H. C. Zhu, H. J. Xu, X. D. Shan, Z. M. Liao, D. P. Yu, *J Phys Chem C* **2009**, *113*, 6450.

[79] Y. F. Li, Z. P. Zhang, G. F. Zhang, L. Zhao, S. Z. Deng, N. S. Xu, J. Chen, *Acs Appl Mater Inter* **2017**, *9*, 3911; Z. P. Zhang, X. M. Song, Y. C. Chen, J. C. She, S. Z. Deng, N. S. Xu, J. Chen, *J Alloy Compd* **2017**, *690*, 304.

[80] C. L. Cheng, Y. F. Chen, R. S. Chen, Y. S. Huang, *Appl Phys Lett* **2005**, *86*.

[81] D. H. Kim, H. R. Lee, M. W. Lee, J. H. Lee, Y. H. Song, J. G. Jee, S. Y. Lee, *Chem Phys Lett* **2002**, *355*, 53.

[82] E. E. Windsor, *Proceedings of the Institution of Electrical Engineers-London* **1969**, *116*, 348; M. Futamoto, S. Hosoki, H. Okano, U. Kawabe, *Journal of Applied Physics* **1977**, *48*, 3541; H. Nagata, K. Harada, R. Shimizu, *Journal of Applied Physics* **1990**, *68*, 3614; K. C. Qi, Z. L. Lin, W. B. Chen, G. C. Cao, J. B. Cheng, X. W. Sun, *Appl Phys Lett* **2008**, *93*; M. Nakamoto, K. Fukuda, *Appl. Surf. Sci.* **2002**, *202*, 289.

[83] H. Zhang, J. Tang, L. Zhang, B. An, L.-C. Qin, *Appl Phys Lett* **2008**, *92*; M. Futamoto, T. Aita, U. Kawabe, *Materials Research Bulletin* **1979**, *14*, 1329; V. V. Morozov, V. I. Malnev, S. N. Dub, P. I. Loboda, V. S. Kresanov, *Inorg. Mater.* **1984**, *20*, 1225.

[84] H. Zhang, J. Tang, J. Yuan, J. Ma, N. Shinya, K. Nakajima, H. Murakami, T. Ohkubo, L. C. Qin, *Nano Lett.* **2010**, *10*, 3539.

[85] H. Zhang, J. Tang, Q. Zhang, G. P. Zhao, G. Yang, J. Zhang, O. Zhou, L. C. Qin, *Adv. Mater.* **2006**, *18*, 87.

[86] H. Zhang, J. Tang, J. S. Yuan, Y. Yamauchi, T. T. Suzuki, N. Shinya, K. Nakajima, L. C. Qin, *Nat. Nanotechnol.* **2016**, *11*, 273.

[87] A. A. Balandin, S. Ghosh, W. Bao, I. Calizo, D. Teweldebrhan, F. Miao, C. N. Lau, *Nano Lett.* **2008**, *8*, 902; A. K. Geim, K. S. Novoselov, *Nature Materials* **2007**, *6*, 183; K. S. Novoselov, A. K. Geim, S. V. Morozov, D. Jiang, M. I. Katsnelson, I. V. Grigorieva, S. V. Dubonos, A. A. Firsov, *Nature* **2005**, *438*, 197.

[88] D. Ye, S. Moussa, J. D. Ferguson, A. A. Baski, M. S. El-Shall, *Nano Lett.* **2012**, *12*, 1265; S. Lv, Z. Li, J. Liao, G. Wang, M. Li, W. Miao, *Scientific Reports* **2015**, *5*; Z. Yang, Q. Zhao, Y. Ou, W. Wang, H. Li, D. Yu, *Appl Phys Lett* **2012**, *101*.

[89] A. T. T. Koh, Y. M. Foong, Z. Yusop, M. Tanemura, D. H. C. Chua, *Advanced Materials Interfaces* **2014**, *1*.

[90] L. Jiang, T. Yang, F. Liu, J. Dong, Z. Yao, C. Shen, S. Deng, N. Xu, Y. Liu, H.-J. Gao, *Adv. Mater.* **2013**, *25*,

250.

[91] G. Eda, H. E. Unalan, N. Rupesinghe, G. A. J. Amaratunga, M. Chhowalla, *Appl Phys Lett* **2008**, *93*.

[92] N. G. Shang, C. P. Li, W. K. Wong, C. S. Lee, I. Bello, S. T. Lee, *Appl Phys Lett* **2002**, *81*, 5024; A. N. Obraztsov, A. P. Volkov, A. A. Zakhidov, D. A. Lyashenko, Y. V. Petrushenko, O. P. Satanovskaya, *Appl. Surf. Sci.* **2003**, *215*, 214; J. J. Wang, M. Y. Zhu, R. A. Outlaw, X. Zhao, D. M. Manos, B. C. Holloway, V. P. Mammana, *Appl Phys Lett* **2004**, *85*, 1265; J. J. Wang, M. Y. Zhu, X. Zhao, R. A. Outlaw, D. M. Manos, B. C. Holloway, C. Park, T. Anderson, V. P. Mammana, *J Vac Sci Technol B* **2004**, *22*, 1269; S. K. Srivastava, A. K. Shukla, V. Vankar, V. Kumar, *Thin Solid Films* **2005**, *492*, 124; M. Y. Chen, C. M. Yeh, J. S. Syu, J. Hwang, C. S. Kou, *Nanotechnology* **2007**, *18*.

[93] Z. S. Wu, S. F. Pei, W. C. Ren, D. M. Tang, L. B. Gao, B. L. Liu, F. Li, C. Liu, H. M. Cheng, *Adv. Mater.* **2009**, *21*, 1756.

[94] A. Malesevic, R. Kemps, A. Vanhulsel, M. P. Chowdhury, A. Volodin, C. Van Haesendonck, *Journal of Applied Physics* **2008**, *104*, 5.

[95] U. A. Palnitkar, R. V. Kashid, M. A. More, D. S. Joag, L. S. Panchakarla, C. N. R. Rao, *Appl Phys Lett* **2010**, *97*, 3.

[96] G. T. Wu, X. L. Wei, S. Gao, Q. Chen, L. M. Peng, *Nat. Commun.* **2016**, *7*; G. T. Wu, X. L. Wei, Z. Y. Zhang, Q. Chen, L. M. Peng, *Adv Funct Mater* **2015**, *25*, 5972.

[97] B. Radisavljevic, A. Radenovic, J. Brivio, V. Giacometti, A. Kis, *Nat. Nanotechnol.* **2011**, *6*, 147; Z. Yin, H. Li, H. Li, L. Jiang, Y. Shi, Y. Sun, G. Lu, Q. Zhang, X. Chen, H. Zhang, *Acs Nano* **2012**, *6*, 74.

[98] A. Castellanos-Gomez, M. Poot, G. A. Steele, H. S. J. van der Zant, N. Agrait, G. Rubio-Bollinger, *Nanoscale Research Letters* **2012**, *7*, 1.

[99] K. F. Mak, C. Lee, J. Hone, J. Shan, T. F. Heinz, *Phys Rev Lett* **2010**, *105*.

[100] Y. B. Li, Y. Bando, D. Golberg, *Appl Phys Lett* **2003**, *82*, 1962.

[101] R. V. Kashid, D. J. Late, S. S. Chou, Y. K. Huang, M. De, D. S. Joag, M. A. More, V. P. Dravid, *Small* **2013**, *9*, 2730.

[102] W. A. Clay, Z. Liu, W. Yang, J. D. Fabbri, J. E. Dahl, R. M. K. Carlson, Y. Sun, P. R. Schreiner, A. A. Fokin, B. A. Tkachenko, N. A. Fokina, P. A. Pianetta, N. Melosh, Z.-X. Shen, *Nano Lett.* **2009**, *9*, 57; W. L. Yang, J. D. Fabbri, T. M. Willey, J. R. I. Lee, J. E. Dahl, R. M. K. Carlson, P. R. Schreiner, A. A. Fokin, B. A. Tkachenko, N. A. Fokina, W. Meevasana, N. Mannella, K. Tanaka, X. J. Zhou, T. van Buuren, M. A. Kelly, Z. Hussain, N. A. Melosh, Z. X. Shen, *Science* **2007**, *316*, 1460.

[103] A. A. Fokin, L. V. Chernish, P. A. Gunchenko, E. Y. Tikhonchuk, H. Hausmann, M. Serafin, J. E. P. Dahl, R. M. K. Carlson, P. R. Schreiner, *Journal of the American Chemical Society* **2012**, *134*, 13641; P. R. Schreiner, L. V. Chernish, P. A. Gunchenko, E. Y. Tikhonchuk, H. Hausmann, M. Serafin, S. Schlecht, J. E. P. Dahl, R. M. K. Carlson, A. A. Fokin, *Nature* **2011**, *477*, 308.

[104] T. M. Willey, C. Bostedt, T. van Buuren, J. E. Dahl, S. G. Liu, R. M. K. Carlson, L. J. Terminello, T. Moller, *Phys Rev Lett* **2005**, *95*.

[105] W. Zhu, G. P. Kochanski, S. Jin, *Science* **1998**, *282*, 1471.

[106] G. Witte, C. Woll, *J. Mater. Res.* **2004**, *19*, 1889; R. J. Maurer, V. G. Ruiz, J. Camarillo-Cisneros, W. Liu, N. Ferri, K. Reuter, A. Tkatchenko, *Prog. Surf. Sci.* **2016**, *91*, 72.

[107] D. Shafir, H. Soifer, B. D. Bruner, M. Dagan, Y. Mairesse, S. Patchkovskii, M. Y. Ivanov, O. Smirnova, N. Dudovich, *Nature* **2012**, *485*, 343; A. S. Landsman, U. Keller, *Phys Rep* **2015**, *547*, 1.

[108] H. Yanagisawa, S. Schnepp, C. Hafner, M. Hengsberger, D. E. Kim, M. F. Kling, A. Landsman, L. Gallmann, J. Osterwalder, *Scientific Reports* **2016**, *6*.

[109] R. G. Hobbs, Y. Yang, A. Fallahi, P. D. Keathley, E. De Leo, F. X. Kartner, W. S. Graves, K. K. Berggren,

Acs Nano **2014**, *8*, 11474.

[110] M. Schultze, K. Ramasesha, C. D. Pemmaraju, S. A. Sato, D. Whitmore, A. Gandman, J. S. Prell, L. J. Borja, D. Prendergast, K. Yabana, D. M. Neumark, S. R. Leone, *Science* **2014**, *346*, 1348; A. Schiffrin, T. Paasch-Colberg, N. Karpowicz, V. Apalkov, D. Gerster, S. Muhlbrandt, M. Korbman, J. Reichert, M. Schultze, S. Holzner, J. V. Barth, R. Kienberger, R. Ernstorfer, V. S. Yakovlev, M. I. Stockman, F. Krausz, *Nature* **2013**, *493*, 70; T. Higuchi, C. Heide, K. Ullmann, H. B. Weber, P. Hommelhoff, *Nature* **2017**, *550*, 224.

[111]A. Autere, H. Jussila, Y. Y. Dai, Y. D. Wang, H. Lipsanen, Z. P. Sun, *Adv. Mater.* **2018**, *30*.

[112] M. Schenk, M. Krueger, P. Hommelhoff, *Phys Rev Lett* **2010**, *105*.

[113] S. Thomas, G. Wachter, C. Lemell, J. Burgdoerfer, P. Hommelhoff, *New Journal of Physics* **2015**, *17*.

[114] M. Krueger, S. Thomas, M. Foerster, P. Hommelhoff, *J Phys B-at Mol Opt* **2014**, *47*.

[115] M. R. Bionta, S. J. Weber, I. Blum, J. Mauchain, B. Chatel, B. Chalopin, *New Journal of Physics* **2016**, *18*.

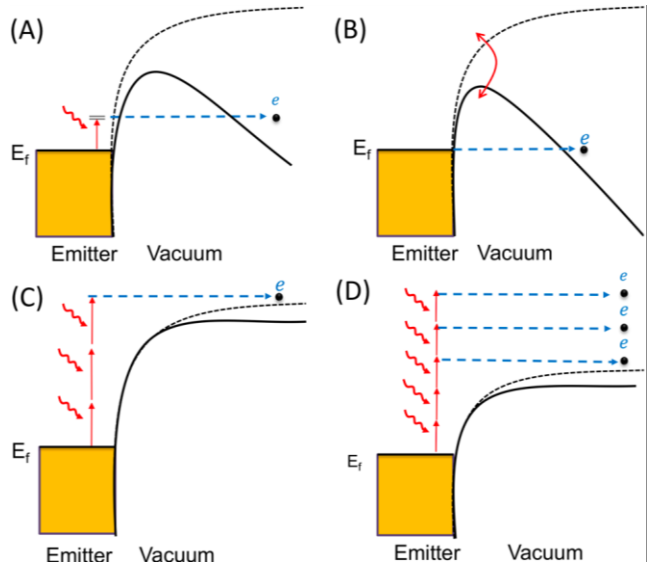

Figure 1. Mechanisms of photoemission. (A) Photofield emission. An electron is excited to an intermediate state when gaining the energy of a photon and then tunnels through the barrier. (B) Optical field emission. When fields is high enough to create a penetrable tunneling barrier, electrons tunnel from the Fermi level. (C) Multiphoton photoemission. Electrons are emitted over the barrier. (D) Above-threshold photoemission. More than the minimum required number of photons is absorbed.

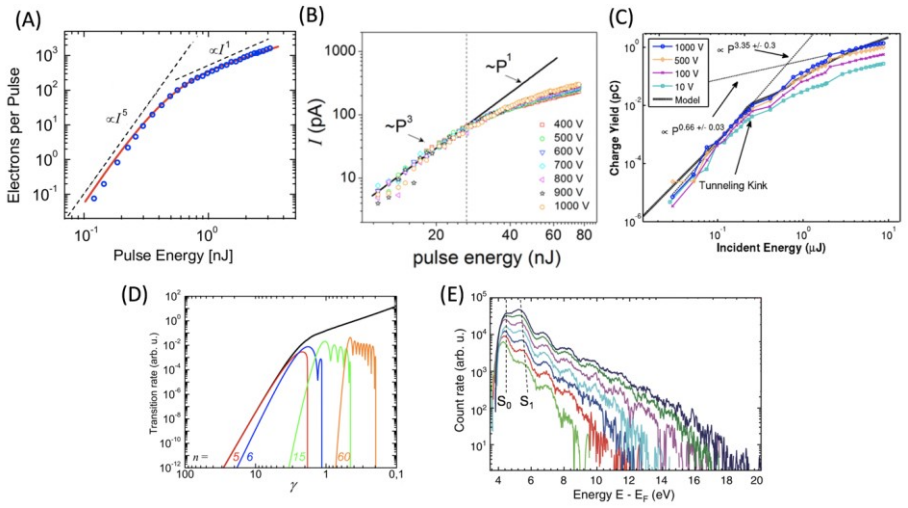

Figure 2. Transition from the multiphoton to the optical tunneling regime. A) Pulse energy dependence of electron current (circles), fifth-order power law (dotted grey) and strong-field approximation model [solid (red)].[37] B) Log-log plot of emission current *vs* pulse energy (P) for a 1 μm pitch square array of Au nanorods for various applied anode bias values. Emission current scales as P^3 up to a pulse energy value of 27 nJ (dashed line).[109] C) Emitted charge and overall quantum efficiency as a function of laser pulse energy for various anode bias voltages. A 3-photon emission growth is shown in current at low intensities, followed by a tunneling kink at an enhanced peak intensity near 1×10^{13} W/cm^2.[40] D) Transition rate for single channels [grey (color)] and total sum (solid black) as a function of Keldysh parameter.[37] E) Electron count rate as a function of the electron energy. From bottom to top the curves are taken at laser intensities of (0.9, 1.2, 1.4, 1.6, 1.9, 2.1, 2.3) × 10^{11} W/cm^2.[112] Reproduced with permission.[37, 40, 109, 112] Copyright 2011, Nature Publishing Group; Copyright 2011, American Chemical Society's Publication; Copyright 2010, American Physical Society's publication.

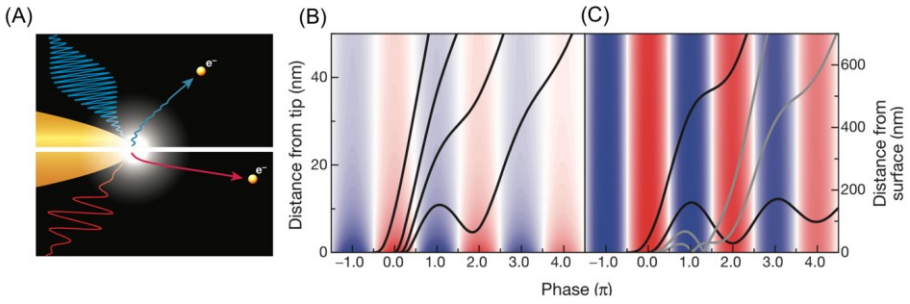

Figure 3. Sub-optical-cycle acceleration regime. A) Trajectories of photoelectrons generated by intense optical fields depend strongly on whether the quiver amplitude is smaller (top, short-wavelength excitation) or larger (bottom, long-wavelength excitation) than the characteristic decay length of the optical near-field (bright white region).[17] B-C) Simulated electron trajectories for four emission phases in localized (B) and homogeneous (C) pulsed fields (wavelength 8 mm, colour shading indicates field; red and blue indicate positive and negative electric force on electron, respectively). Grey lines are rescattered trajectories.[17] Reproduced with permission. [17] Copyright 2012, Nature Publishing Group

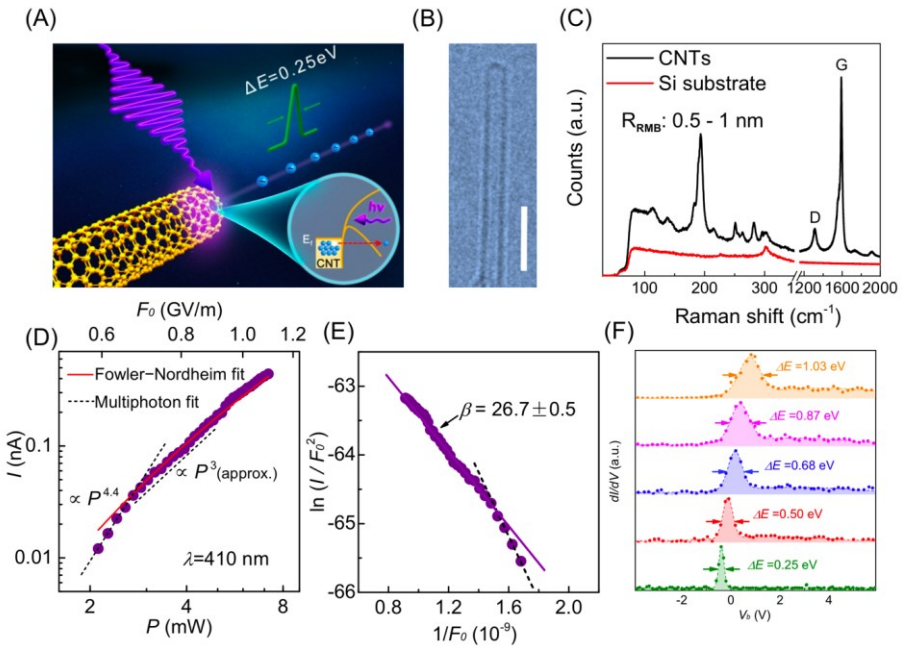

Figure 4. Highly coherent CNT-based photoemission source. A) Emission dynamics.[44] B) High resolution transmission electron microscopy image of a typical CNT under study. Scale bar: 5 nm.[44] C) Raman spectrum of the CNTs, indicates a radius of 0.5-1 nm. D) Emission current as a function of laser power (P) (bottom abscissa) and laser feld (F_0) (top abscissa) at bias voltage (V_b) of 50 V. At low power range, multiphoton regime is noted, while feld-driven regime is noted at higher power range.[44] E) FN plot of the optically driven emission current, showing a feld enhancement factor (β) of 26.7 ± 0.5.[44] F) corresponding dI/dV curves; the width of the peaks (FWHM) indicates the energy spreads (ΔE), while the shoulder indicates the beam divergence grade.[44]

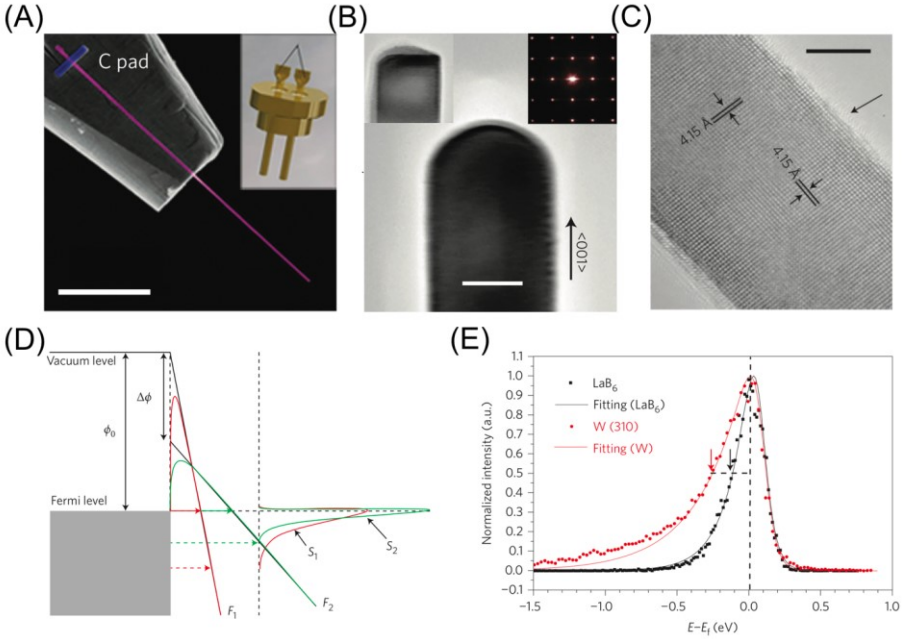

Figure 5. LaB_6 nanowire field emitter. A) SEM image showing the finished LaB_6 nanowire emitter and the complete emitter assembly used for field-emission SEM.[86] B) Hemispherical nanowire tip produced by field evaporation. Scale bar: 30 nm. Left inset: assembled tip. Right inset: the electron diffraction pattern of the tip after field evaporation, showing that perfect crystallinity is maintained.[86] C) High-resolution TEM image showing the clean surface of the LaB_6 nanowire synthesized by this method. Scale bar:5 nm.[86] D) Energy band showing the origin of the low work function for a LaB_6 nanowire and its influence on emission current density and beam monochromaticity.[86] E) Electron energy distribution from a LaB_6 nanowire and a W(310) tip emitting at current densities of 1.8×10^{10} A m^{-2} and 3.6×10^{9} A m^{-2}, respectively.[86] Reproduced with permission. [86] Copyright 2015, Nature Publishing Group

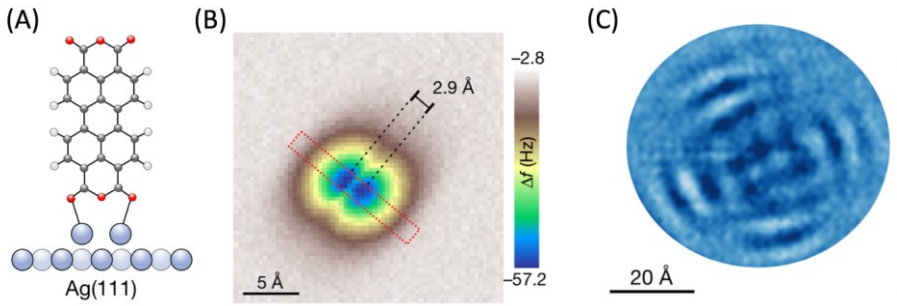

Figure 6. Single molecule field emitter. A) Schematic side view of a standing PTCDA molecule.[12] B) AFM image of the standing molecule, recorded at $z = 17.5$ Å.[12] C) Successive field-emission images (without the background).[12] Reproduced with permission.[12] Copyright 2018, Nature Publishing Group

Table 1. Typical ultrafast field emission materials and their key parameters.

Materials	Morphology	Size of the emitting tip	Substrate	Field enhancement (wavelength)	Dominant field enhancement mechanism	The local optical field strength (when access strong field emission)
gold	nanowire[50]	90 nm-190 nm[50]	Tungsten tips[50]	Simulation:6.6-10.4 (750 nm)[50] Experiment:5.98 ± 0.24 (750 nm)[50]	Geometry effect[50]	23 V/nm[50]
	nanosphere[51]	90 nm[51]	Si[51]	1000 (780 nm)[51]	Plasmon resonance[51]	50 V/nm[51]
	nanorod[53, 54]	150 nm×50 nm[53] 70 nm×20 nm[54]	ZnS[53] ITO[54]	36 (500 nm)[53] 60 (800 nm)[54]	Plasmon resonance[53, 54]	3.5 V/nm[53] 3-4.3 V/nm[54]
	nanotip[17]	10 nm[17]	–	10 (800 nm)[17]	Plasmon resonance and geometry effect[17]	28 V/nm[17]
	nanotriangle[42]	(160-300 nm× 120-225 nm)[42]	ITO[42]	32 (1177 nm)[42]	Plasmon resonance[42]	40 V/nm[42]
tungsten	nanotip[113, 114]	5 nm[113] 8-51 nm[114]	–	12 (800 nm)[113] 2.6-5.7 (800 nm)[114]	Geometry effect[113, 114]	– 8.7 V/nm[114]
silicon	pillar[40]	4.4 nm[40]	–	10.5 (800nm)[40]	Geometry effect[40]	8.7 V/nm[40]
silver	nanotip[115]	12-50 nm[115]	–	3.8±0.1 (800 nm)[115] 12.2±2 (400 nm)[115]	Plasmon resonance and geometry effect[115]	2.7 V/nm[115]
dielectric	nanosphere[61, 63]	100 nm[63] 52-147 nm[61]	–	1.3 (720 nm)[63] 1.54 (720 nm)[61]	Geometry effect[61, 63]	15 V/nm[63] 12.3 V/nm[61]
Carbon nanotube	nanotip[44]	0.5-1 nm[44]	–	26.7±0.5 (410 nm)[44]	Geometry effect[44]	0.66 V/nm[44]

WILEY-VCH